J Pharmacol Sci **107**, 80 – 89 (2008)

Journal of Pharmacological Sciences

Full Paper

Effects of Atorvastatin and Pravastatin on Signal Transduction Related to Glucose Uptake in 3T3L1 Adipocytes

Akira Takaguri[1], Kumi Satoh[1,*], Mai Itagaki[1], Yukiko Tokumitsu[2], and Kazuo Ichihara[1]

[1]*Division of Pharmacology, Hokkaido Pharmaceutical University School of Pharmacy, 7-1 Katsuraoka, Otaru 047-0264, Japan*
[2]*Laboratory of Clinical Pharmacology, Department of Clinical Pharmacy, Faculty of Pharmaceutical Sciences, Aomori University, Aomori 030-0943, Japan*

Received December 21, 2007; Accepted March 25, 2008

Abstract. A number of patients with hyperlipidemia are prescribed 3-hydroxy-3-methylglutaryl-CoA reductase inhibitors that are concomitantly used along with the treatment of diabetes mellitus. The effects of atorvastatin and pravastatin on insulin-induced glucose uptake and the related signal transduction in 3T3L1 adipocytes were studied. 3T3L1 fibroblasts were differentiated into adipocytes, pretreated with atorvastatin or pravastatin, and then exposed to insulin. Glucose uptake and the amount of insulin signal proteins were measured. Atorvastatin significantly decreased insulin-stimulated 2-deoxyglucose uptake in 3T3L1 adipocytes associated with the prevention of translocation of GLUT4 into the plasma membrane. The amounts of Rab4 and RhoA that required lipid modification with farnesyl or geranylgeranyl pyrophosphate, in the membrane fraction were decreased by atorvastatin. Insulin-induced tyrosine phosphorylation of IRS-1 and serine/threonine phosphorylation of Akt were reduced by atorvastatin. Pravastatin did not modify these insulin-induced changes in the signal transduction. Inhibitors of the RhoA/Rho kinase system, C3 and Y27632, as well as atorvastatin reduced insulin-induced changes in signal transduction. Atorvastatin and pravastatin did not affect messenger RNA expression, protein level, and tyrosine phosphorylation of insulin receptors. In conclusion, hydrophobic atorvastatin decreases the glucose uptake by 3T3L1 adipocytes since it can enter the cell and prevents lipid modification of some proteins that are involved in the insulin signal transduction process.

Keywords: adipocyte, insulin, glucose, 3-hydroxy-3-methylglutaryl-CoA (HMG-CoA) reductase, signal transduction

Introduction

In the insulin-sensitive tissue cells (e.g., skeletal muscle and fat tissue), insulin signal transduction starts with the binding of insulin to insulin receptors (IR) and ends with the translocation of glucose transporter-4 (GLUT4) from intracellular vesicles to the plasma membrane. Extracellular glucose is incorporated into the cell via the GLUT4 in the plasma membrane. Various factors are involved in the insulin signal transduction process, including insulin receptor substrate-1 (IRS-1), phosphatidylinositol 3-kinase, and Akt (1 – 3). Some small GTP-binding proteins (G-proteins) also play an important role in this process. Rab4 is involved in the intracellular vesicle transport system, such as translocation of GLUT4 (4). RhoA and Rho-kinase modulates the activities of IRS-1 (5).

3-Hydroxy-3-methylglutaryl-CoA (HMG-CoA) reductase inhibitors (such as statins) lower the concentrations of low-density lipoprotein cholesterol in blood and are widely used in patients with hypercholesterolemia or hyperlipidemia (6). Statins are taken by some diabetic patients since a number of hypercholesterolemic patients have diabetes mellitus. Diabetic patients treated with simvastatin and atorvastatin have safety characteristics similar to that of non-diabetic patients (7). Statins also improve insulin resistance by lowering plasma triglyceride concentration in non-insulin-dependent dia-

*Corresponding author. kumi@hokuyakudai.ac.jp
Published online in J-STAGE on May 9, 2008 (in advance)
doi: 10.1254/jphs.FP0072403

betic patients (8). Cerivastatin improves insulin secretion and increases insulin-mediated glucose uptake in the early stage of obese type-II diabetes (9). In an experimental study, simvastatin protected against low-dose streptozotocin-induced diabetes in mice (10). These findings enable physicians to prescribe statin for hypercholesterolemic patients with diabetes. On the other hand, experimental studies indicate that statins may disturb the insulin signal transduction process. Lovastatin disrupts the early events in insulin signaling (11), whereas simvastatin suppresses glucose-induced insulin release from the rat islet β-cells in vitro (12). Moreover, we also have demonstrated that atorvastatin worsens glucose tolerance in streptozotocin-induced diabetic rats in vivo (13). These findings may suggest that statins aggravate the function of insulin in diabetic patients. HMG-CoA reductase is the rate-limiting enzyme in the mevalonic pathway. This provides isoprenoids such as farnesyl and geranylgeranyl pyrophosphates for the post-translational lipid modification of several proteins including the small G-proteins involved in the insulin signal transduction. Statins must therefore affect the pathogenesis of diabetes or the response to insulin. The precise mechanism of action of statins and how insulin function is improved or exacerbated in insulin-sensitive cells is unclear. Thus, the aim of the present study was to examine the effects of atorvastatin and pravastatin on glucose uptake and the insulin signal transduction process in 3T3L1 adipocytes.

Materials and Methods

Drugs and reagents

Pravastatin and atorvastatin were kindly provided by Sankyo Company (Tokyo). Aporotinin, leupeptin, phenylmethanesulphonylfluoride (PMSF), *dl*-mevalonic acid lactone, and bovine serum albumin (BSA) were purchased from Sigma (St. Louis, MO, USA). Dulbecco's modified Eagle's medium (DMEM), phloridzin, $HgCl_2$, isobutylmethylxanthine (IBMX), and dexamethasone were purchased from Wako (Osaka). The DC protein assay kit and sodium dodecyl sulfate (SDS) were from Bio-Rad (Hercules, CA, USA). Insulin was from Novo Nordisk (Bagsværd, Denmark). Protein A-Sepharose and [1,2-^{3}H]2-DG were from Amersham Pharmacia Biotech (Piscataway, NJ, USA). Exoenzyme C3 and Y27632 were from Calbiochem (San Diego, CA, USA). Aquasol II was from PerkinElmer (Waltham, MA, USA). Fetal bovine serum (FBS), TRIzol reagent and Superscript™ III First-Strand were from Invitrogen (Carlsbad, CA, USA). The PerfectShot Taq kit was from Takara Biomedicals (Tokyo). COD-Star Reagent was obtained from New England BioLabs (Ipswich, MA, USA). Anti-phospho-IGF-IF (Tyr1131) / insulin receptor (Tyr1146) antibody, anti-IRS-1, anti-phospho-Akt (308), anti-phospho-Akt (473), and anti-mouse and anti-rabbit immunoglobulin G secondary antibodies were purchased from Cell Signaling Technology (Bevery, MA, USA). Anti-RhoA, anti-Rab4, and anti-Glut4 antibodies were from Santa Cruz Biotechnology (Santa Cruz, CA, USA). Anti-phosphotyrosine (PY20) antibody was from BD Transduction Laboratories (Lexington, KY, USA).

Cell culture

3T3L1 fibroblasts were obtained from Health Science Research Resources Bank (Osaka) and grown in DMEM high glucose containing 10% FBS at 37°C in a humidified atmosphere of 5% CO_2. Three days after confluence, the cells were incubated to allow differentiation into adipocytes in DMEM high glucose containing 10% FBS, 100 mU/ml insulin, 0.5 mM IBMX and 250 nM dexamethasone for 3 days and then incubated for a further 3 days in the medium without IBMX and dexamethasone. The cells were further allowed to incubate in the DMEM high glucose containing 10% FBS until use. The medium was changed every 3 days. 3T3L1 adipocytes were used for experiments between 12 – 16 days after initiation of differentiation. Cells were pretreated with either atorvastatin or pravastatin at 1, 5, or 10 μM for 24 or 72 h and then exposed to insulin at the concentrations of 0.1 or 1 μM for the period as indicated.

Glucose uptake

3T3L1 adipocytes on 6 well plates were incubated in FBS-free DMEM low glucose for 16 h. Cells were washed with Krebs Ringer phosphate (KRP)-HEPES buffer (25 mM HEPES pH 7.4, 118 mM NaCl, 4.7 mM KCl, 2.5 mM $CaCl_2$, 1.2 mM $MgSO_4$, and 1 mM KH_2PO_4) containing 1% BSA and then incubated for 10 min with or without 1 μM insulin. Unlabeled and labeled 0.1 mM of 2-deoxyglucose (0.5 μCi) was added to each well. After 10 min, the reaction was stopped by adding 1 mM $HgCl_2$ and 0.2 mM phloridzin. Cells were rapidly washed three times with ice-cold phosphate-buffered saline (PBS) and were solubilized in 1 ml 5% SDS. Radioactivity was measured by a liquid scintillation counter.

Preparation of plasma membrane for GLUT4 immunoblotting

3T3L1 adipocytes were fractionated by ultracentrifugation to separate the cytosol and plasma membrane contents according to the method described by Knight et al. (14). The cells on 100-mm dishes were washed three times with ice-cold PBS and scraped into 1 ml TES buffer (10 mM Tris pH 7.5, 250 mM sucrose, and 1 mM

EDTA) containing 1 mM sodium vanadate, 1 mM PMSF, 10 μg/ml aprotinin, and 10 μg/ml leupeptine. Samples were homogenized (20 strokes in a Teflon™ homogenizer), and centrifuged at 16,000 × *g* for 15 min. The pellet was resuspended and centrifuged at 16,000 × *g* again. The resulting pellet consisted of nuclei, mitochondria, and plasma membrane. Plasma membrane fragments were isolated as follows: the 16,000 × *g* pellet was homogenized (20 strokes) in TES buffer, layered on a 1.15 M sucrose cushion (TES buffer containing 1.15 M sucrose), and centrifuged at 100,000 × *g* in swing rotor for 60 min. The white fluffy band at the interface was collected, diluted in TES, and centrifuged again at 48,000 × *g* for 60 min, yielding a pellet of the plasma membrane. The amount of GLUT4 in the plasma membrane was determined by immunoblotting using anti-GLUT4 antibody.

IR mRNA expression

Total RNA from 3T3L1 adipocytes was extracted with TRIzol reagent. Total RNA of 1.5 μg was reverse transcribed with Superscript™ III First-Strand. The resulting cDNA was amplified using the PerfectShot Taq kit. Sense and antisense primers for IR were 5'-CCAACCATCTGTAAGTCACA-3' and 5'-ACATCAA GTTGCTGGAATTCATG-3', respectively. β-Actin mRNA was also amplified. After reverse transcriptase polymerase chain reaction (RT-PCR), a sample from each reaction tube was subjected to electrophoresis on 1.5% agarose gels containing 1% ethidium bromide.

Immunoprecipitation and immunoblotting of IRS-1

3T3L1 adipocytes on 100-mm plates were washed three times with ice-cold PBS and scraped into 0.5 ml lysis buffer (25 mM Tris pH 7.5, 150 mM NaCl, 10 mM sodium fluoride, 1 mM sodium vanadate, 1 mM PMSF, 10 μg/ml aprotinin, 10 μg/ml leupeptine, and 1% Nonidet 40). Immunoprecipitation with antiphosphotyrosine antibody (PY20) was performed by incubating the lysates with antibody at 4°C overnight. Immune complexes were collected on protein-A-Sepharose for 3.5 h at 4°C, washed three times with the lysis buffer, and boiled in SDS sample buffer (50 mM Tris, 2% SDS, 10% glycerol, 50 mM dithiothreitol, and 0.1% bromophenol blue). Samples were electrophoresed on 7.5% SDS-polyacryamide gels and transferred to a polyvinylidine difluoride membrane. The membrane was blocked with blocking buffer (PBS, 0.1% Tween 20, 0.5 mM sodium vanadate, 0.02% sodium azide, and 5% nonfat dry milk). For anti-IRS-1 immunoblotting, the membrane was probed with an anti-IRS-1-antibody at 4°C overnight in blocking buffer containing 5% BSA, and incubated with rabbit IgG antibody for 1 h at room temperature. Immunoblots were detected using a COD-Star Reagent.

Immunoblotting of RhoA and Rab4 in cytosol and membrane fractions

3T3L1 adipocytes on 100-mm plates were washed three times with ice-cold PBS and scraped into 300 μl Tris buffer (25 mM Tris pH 7.5, 150 mM NaCl, 10 mM sodium fluoride, 1 mM sodium vanadate, 1 mM PMSF, 10 μg/ml aprotinin, and 10 μg/ml leupeptine). Cells were homogenized (20 strokes) and centrifuged at 500 × *g* for 10 min. The supernatant was centrifuged at 20,000 × *g* for 30 min to separate the cytosolic and crude membrane fractions. Each fraction was probed with anti-RhoA and anti-Rab4 antibodies and immunoblots were detected using a COD-Star Reagent.

Immunoblotting of phosphorylated IR and Akt in membrane fractions

The crude membrane fraction was obtained from 3T3L1 adipocytes as described above and used for immunoblotting of tyrosine phosphorylated IR and serine/threonine phosphorylated Akt.

Statistical analyses

Values are expressed as means ± S.E.M. The significance of the differences between the groups was evaluated using one-way ANOVA followed by Student's or Dunnett's *t* test with Stat View (SAS Institute Inc., Cary, NC, USA). $P<0.05$ was considered statistically significant.

Results

Glucose uptake and GLUT4 translocation

Exposure of 3T3L1 adipocytes to 1 μM insulin for 10 min stimulated 2-deoxyglucose uptake into the cells (Fig. 1A). Pretreatment with 10 μM atorvastatin for 72 h significantly decreased the insulin-stimulated 2-deoxyglucose uptake, whereas that with pravastatin was not affected under identical conditions. Translocation of GLUT4 from intracellular vesicle to the plasma membrane was detected (Fig. 1B) when 3T3L1 adipocytes were treated with 0.1 μM insulin for 30 min. Pretreatment with 1, 5, or 10 μM atorvastatin for 72 h decreased the amount of GLUT4 in the plasma membrane, which was increased by insulin in a concentration-dependent manner. The decrease in the GLUT4 level in the 5 and 10 μM atorvastatin–treated cells was statistically significant compared with that of untreated cells. However, pretreatment with pravastatin did not alter insulin-stimulated GLUT4 translocation to the plasma membrane.

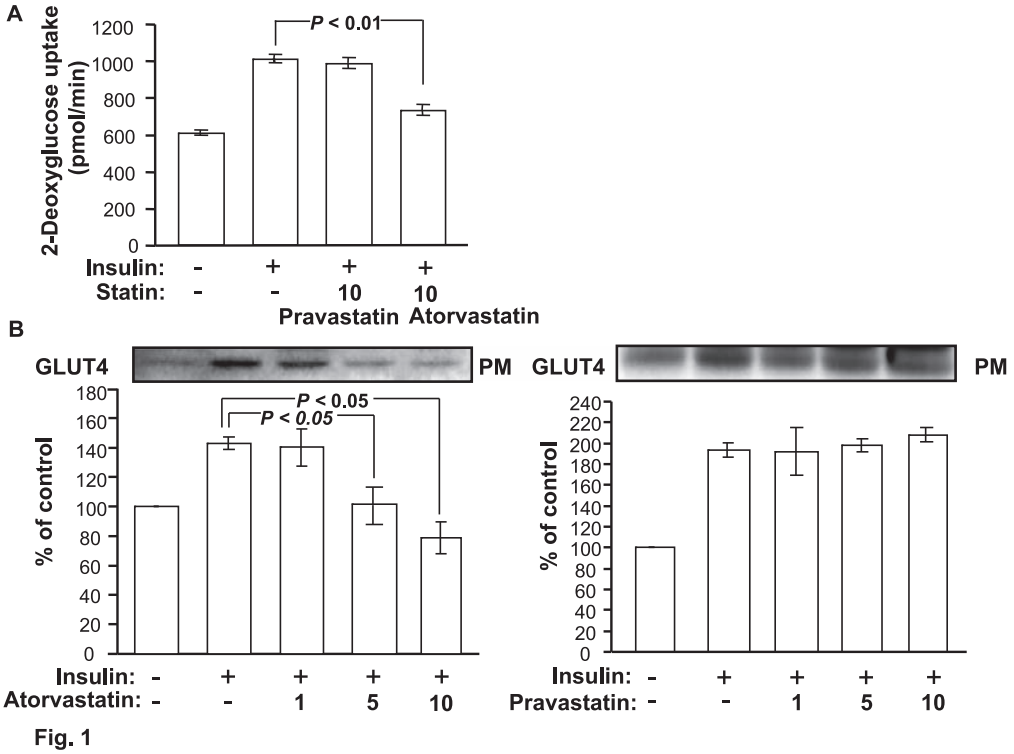

Fig. 1. Effects of pravastatin and atorvastatin on glucose uptake (A) and GLUT4 translocation (B) after exposure of 3T3L1 adipocytes to insulin. A: After pretreatment of 3T3L1 adipocytes with either pravastatin (10 μM) or atorvastatin (10 μM) for 72 h, the cells were exposed to 1 μM insulin for 10 min. After washing with PBS, the [^{3}H]-2-deoxy-D-glucose radioactivity of the cell was measured. Data are expressed as means ± S.E.M. (pmol 2-deoxyglucose uptake/min per well) of three observations. B: After pretreatment of 3T3L1 adipocytes with either pravastatin (1, 5, or 10 μM) or atorvastatin (1, 5, or 10 μM) for 72 h, the cells were exposed to 0.1 μM insulin for 30 min. The plasma membrane of the cell was fractionated, and the GLUT4 was determined by immunoblotting analysis using anti-GLUT4 antibody. The amounts of GLUT4 are expressed as percentage of that in the untreated (control) cells (means ± S.E.M. of three independent observations).

Expression of mRNA expression, protein level, and phosphorylation of IR

Pretreatment with atorvastatin or pravastatin did not alter IR mRNA expression (Fig. 2) and the protein level of IRβ (data not shown) in the absence of insulin. The quantitiy of the IRβ protein under insulin stimulation also was not modified by pretreatment with atorvastatin and pravastatin for 24 h (Fig. 3A). Immunoblot analysis clearly showed tyrosine phosphorylation of IR in the crude membrane fraction 3 min after exposure of 3T3L1 adipocytes to 0.1 μM insulin (Fig. 3B). However atorvastatin or pravastatin did not alter the amount of phosphorylated IR increased by insulin.

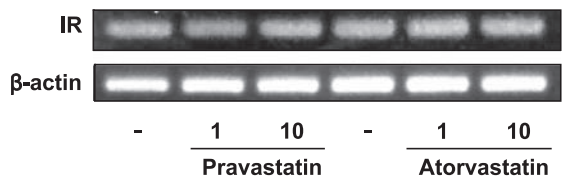

Fig. 2. Effects of pravastatin and atorvastatin on mRNA expression of IR. After pretreatment of 3T3L1 adipocytes with either pravastatin (1 or 10 μM) or atorvastatin (1 or 10 μM) for 24 h, IR mRNA expression was quantified by RT-PCR using β-actin mRNA as the internal standard. A representative expression is shown out of three independent experiments.

Subcellular distribution of Rab4

A certain amount of Rab4 naturally exists in the crude membrane fraction (Fig. 4). Exposure of 3T3L1 adipocytes to 0.1 μM insulin for 30 min did not appreciably affect the amount of Rab4 in the membrane and cytosolic fraction. Pretreatment with 1, 5, or 10 μM atorvastatin for 24 h decreased the amount of Rab4 in the membrane fraction and increased that in the cytosolic fraction in a concentration-dependent manner. Statistically significant differences in the amount of Rab4 were observed in treated cells at a certain concentration of atorvastatin as compared with that in the non-treated cells. The concomitant existence of mevalonic acid completely reversed the changes in the subcellular distribution of Rab4 caused by atorvastatin treatment (two bands of immunoblots in the atorvastatin-treated

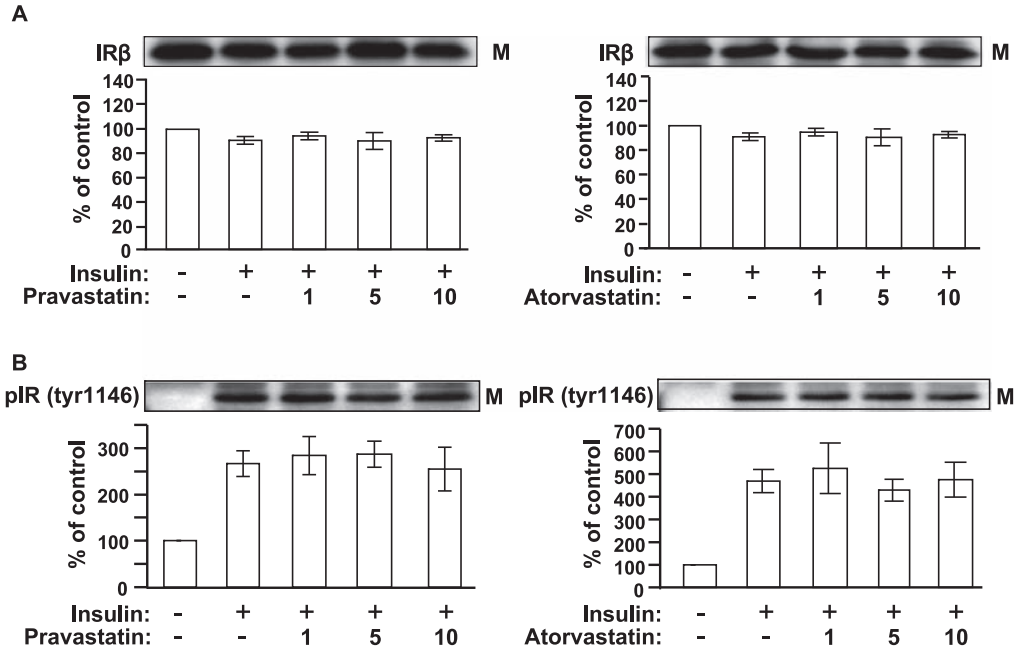

Fig. 3. Effects of pravastatin and atorvastatin on IRβ protein level (A) and on the amount of tyrosine phosphorylated IR (B) in the membrane fraction in the presence of insulin. After pretreatment of 3T3L1 adipocytes with either pravastatin (1, 5, or 10 μM) or atorvastatin (1, 5, or 10 μM) for 24 h, cells were stimulated with 0.1 μM insulin for 3 min. In the crude membrane fraction (M), IRβ protein (A) or tyrosine phosphorylation (B) of IR was determined by immunoblotting analysis. The amounts of IRβ protein and tyrosine-phosphorylated IR are expressed as the percentage of that in the untreated (control) cells (means ± S.E.M. of 3 – 4 independent observations).

cells are seen on the right in Fig. 4). Pravastatin did not appreciably affect the subcellular distribution of Rab4.

Subcellular distribution of RhoA

A certain amount of RhoA naturally exists in the crude membrane fraction (Fig. 5). Stimulation with insulin did not influence the subcellular distribution of RhoA between the membrane and cytosolic fraction. Pravastatin did not modify the distribution of RhoA between the cytosol and plasma membrane. Pretreatment with atorvastatin for 24 h decreased the level of RhoA in the membrane fraction and increased it in the cytosolic fraction in a concentration-dependent manner. The decrease in the RhoA level in the 5 and 10 μM atorvastatin–treated cells and the increase in the level in the 10 μM atorvastatin–treated cells were statistically significant as compared with that in the non-treated cells with atorvastatin.

Phosphorylation of IRS-I and Akt

Exposure of 3T3L1 adipocytes to 0.1 μM insulin for 5 min markedly increased tyrosine phosphorylation of IRS-1 (Fig. 6). Pretreatment with 1, 5, or 10 μM atorvastatin decreased the tyrosine phosphorylation of the IRS-1 in a concentration-dependent manner, whereas pravastatin did not. There was a significant difference in the level of phosphorylated IRS-1 between the non-treated and treated cells with 10 μM atorvastatin. Serine/threonine phosphorylation of Akt in the crude membrane fraction was examined because Akt should exist and function in the plasma membrane or the intracellular vesicle membrane. Exposure of 3T3 L1 adipocytes to 0.1 μM insulin for 10 min obviously phosphorylated serine and threonine residues in Akt (Fig. 7). Pravastatin did not modify the phosphorylation of Akt caused by insulin, whereas atorvastatin significantly decreased the serine/threonine phosphorylation of Akt in a concentration-dependent manner.

C3 toxin and Rho-kinase inhibitor Y27632 on phosphorylation of IRS-1

Treatment with 15 μg/ml C3 exoenzyme of *Clostridium botulinum* (inactivator of RhoA) for 48 h appeared to inhibit insulin-induced tyrosine phosphorylation of IRS-1 (Fig. 8) as well as that of atorvastatin (Fig. 6). Treatment with Y27632 (chemical inhibitor of Rho-kinase) at 100 μM for 24 h significantly inhibited the increase in tyrosine phosphorylation of IRS-1 caused by 0.1 μM insulin exposure (Fig. 9A). Treatment of 3T3L1 adipocytes with 10 μM Y27632 for 72 h also inhibited the insulin-induced translocation of GLUT4 to the plasma membrane (Fig. 9B).

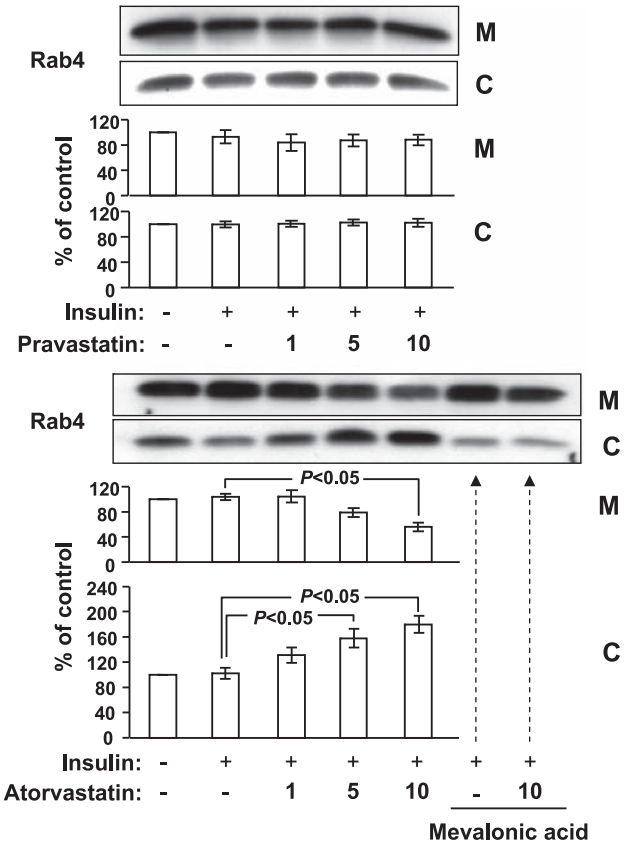

Fig. 4. Effects of pravastatin and atorvastatin on subcellular distribution of Rab4 in the presence of insulin. After pretreatment of 3T3L1 adipocytes with either pravastatin (1, 5, or 10 μM) or atorvastatin (1, 5, or 10 μM) for 24 h, the cells were exposed to 0.1 μM insulin for 30 min. Cells were fractionated into the crude membrane fraction (M) and cytosol (C), and the amount of Rab4 was determined by immunoblotting analysis using anti-Rab4 antibody, which was expressed as the percentage of that in the untreated (control) cells (means ± S.E.M. of 3 – 4 independent observations). Reversal of atorvastatin-induced changes in Rab4 subcellular distribution with 10 μM mevalonic acid is shown on the right side of the immunoblots in the atorvastatin-treated cells.

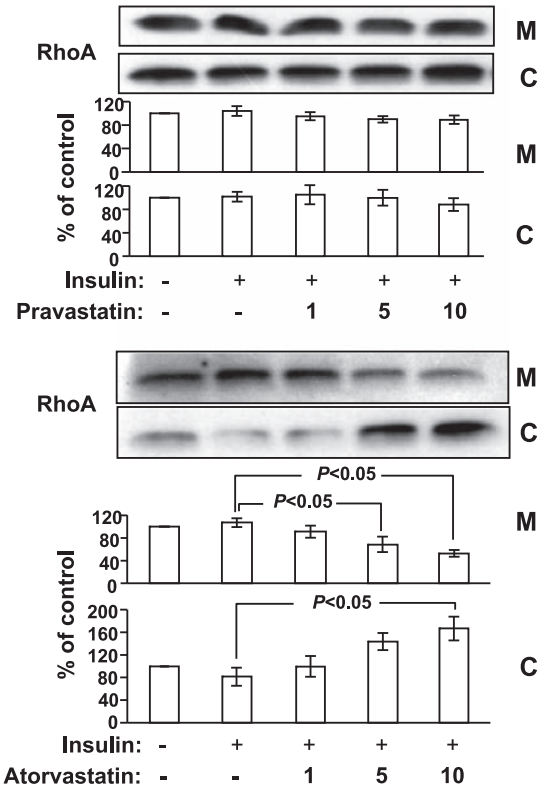

Fig. 5. Effects of pravastatin and atorvastatin on subcellular distribution of RhoA in the presence of insulin. After pretreatment of 3T3L1 adipocytes with either pravastatin (1, 5, or 10 μM) or atorvastatin (1, 5, or 10 μM) for 24 h, the cells were exposed to 0.1 μM insulin for 10 min. RhoA was determined by immunoblotting analysis using anti-RhoA antibody in the membrane fraction (M) and cytosol (C). The amounts of RhoA are expressed as the percentage of that in the untreated (control) cells (means ± S.E.M. of 3 – 4 independent observations).

Discussion

Atorvastatin but not pravastatin significantly reduced glucose uptake induced by insulin treatment in 3T3L1 adipocytes (Fig. 1A). Membrane permeabilities among HMG-CoA reductase inhibitors are different (15). This is because atorvastatain is a hydrophobic compound and can easily enter any cell and inhibits HMG-CoA reductase (16). In contrast, pravastatin is a hydrophilic compound and cannot penetrate extrahepatic cells. However, pravastatin can inhibit HMG-CoA reductase in the hepatic cell (17) because the hepatic plasma membrane contains organic anion transporters that transport hydrophilic substances into the cell. Atorvastatin and pravastatin are therefore equally effective in lowering the concentration of cholesterol in blood.

Isoprenylation of G-proteins with farnesyl or a geranylgeranyl group is an essential process for G-protein function (18). These isoprenyl groups are derived from the mevalonic pathway, in which the HMG-CoA reductase is the rate-limiting enzyme (19). The system may lose its function due to lack of isoprenyl groups caused by HMG-CoA reductase inhibition in 3T3L1 adipocytes since the insulin signal transduction system involves several small G-proteins such as Rab4 and RhoA. Membrane-permeable atorvastatin can affect insulin signal transduction, resulting in attenuation of insulin-induced glucose uptake into 3T3L1 adipocytes, but membrane-impermeable pravastatin cannot.

We showed that decrease in insulin-induced glucose uptake by atorvastatin was associated with decrease in the amount of GLUT4 in the plasma membrane (Fig. 1B). Chamberlain (20) has reported that lovastatin, another hydrophobic statin, also reduces the expression

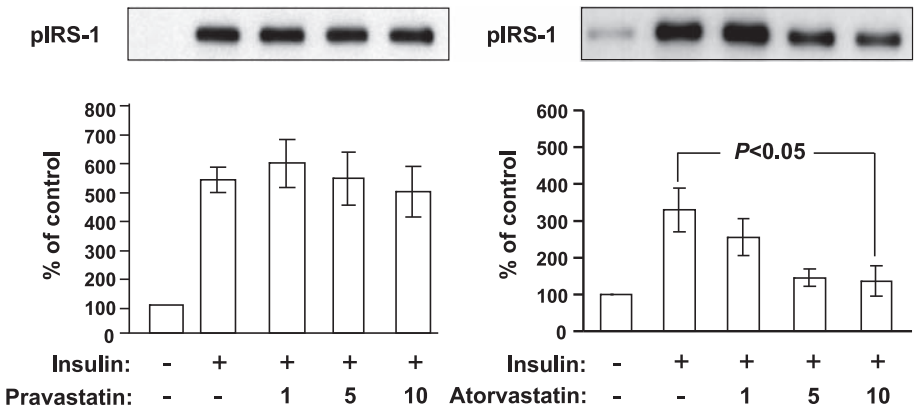

Fig. 6. Effects of pravastatin and atorvastatin on tyrosine phosphorylation of IRS-1 induced by insulin. After pretreatment of 3T3L1 adipocytes with either pravastatin (1, 5, or 10 μM) or atorvastatin (1, 5, or 10 μM) for 24 h, the cells were exposed to 0.1 μM insulin for 5 min. The whole cell lysate was immunoprecipitated with PY20 antibody, separated by SDS-PAGE, and immunoblotted with anti-IRS-1 antibody. The amounts of phosphorylated IRS-1 are expressed as the percentage of that in the untreated (control) cells (means ± S.E.M. of 3 – 4 independent observations).

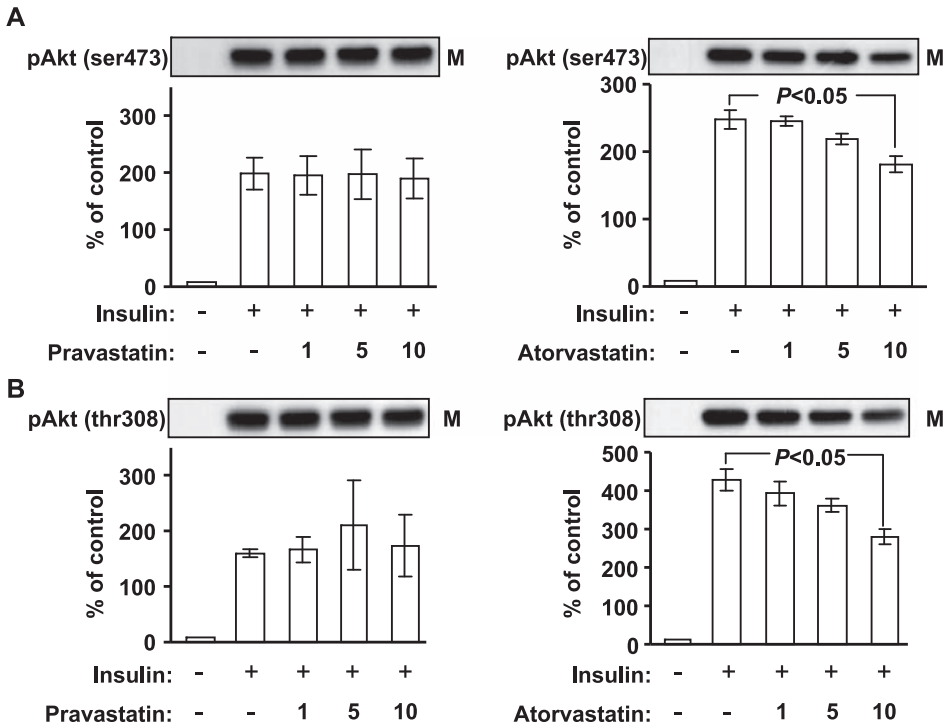

Fig. 7. Effects of pravastatin and atorvastatin on serine (A) and threonine (B) phosphorylation of Akt in the crude membrane fraction induced by insulin. After pretreatment of 3T3L1 adipocytes with either pravastatin (1, 5, or 10 μM) or atorvastatin (1, 5, or 10 μM) for 24 h, the cells were exposed to 0.1 μM insulin for 10 min. In the crude membrane fraction (M), serine (A) and threonine (B) phosphorylation of Akt was determined by immunoblotting analysis using anti-phospho-Akt (308) and anti-phospho-Akt (473). The amounts of phosphorylated Akt are expressed as the percentage of that in the untreated (control) cells (means ± S.E.M. of 3 – 4 independent observations).

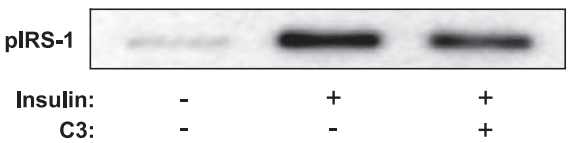

Fig. 8. Effects of C3 toxin on insulin-induced tyrosine phosphorylation of IRS-1. 3T3L1 adipocytes were pretreated with C3 toxin (15 μg/mL) for 48 h and exposed to 0.1 μM insulin for 5 min. The whole cell lysate was immunoprecipitated with PY20 antibody, and immunoblotted with anti-IRS-1 antibody.

of GLUT4 in the total membrane fraction of 3T3L1 adipocytes in the absence of insulin, and it inhibits the insulin-induced glucose uptake into the cell. However, he did not describe the precise mechanism by which lovastatin inhibits GLUT4 translocation and glucose uptake. Attenuation of insulin-induced translocation of GLUT4 from intracellular vesicles to the plasma membrane by atorvastatin is not due to IR (Figs. 2 and 3) but because of the intracellular signal transduction process of insulin (Fig. 10).

Rab4, a small G-protein, is involved in the mechanism of GLUT4 translocation to the plasma membrane (4, 21). Rab4 also requires an isoprenyl group to anchor to the membrane when it is activated. Atorvastatin converted the localization of Rab4 in the presence of insulin from the membrane to the cytosolic fraction in a concentration-dependent manner (Fig. 4). It is likely that

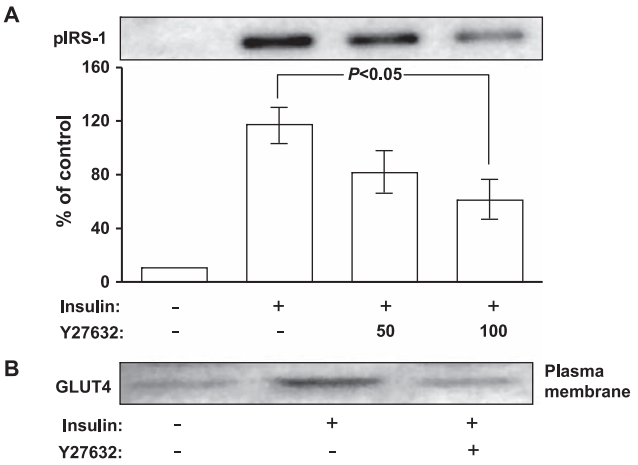

Fig. 9. Effects of Y27632, a Rho-kinase inhibitor, on insulin-induced tyrosine phosphorylation of IRS-1 (A) and GLUT4 translocation to the plasma membrane (B). A: 3T3L1 adipocytes were pretreated with 50 and 100 μM Y27632 for 24 h, and then exposed to 0.1 μM insulin for 5 min. Whole cell lysate was immunoprecipitated and immunoblotted. The amounts of phosphorylated IRS-1 are expressed as the percentage of that in the untreated (control) cells (means ± S.E.M. of 3 – 4 independent observations). B: 3T3L1 adipocytes were pretreated with 10 μM Y27632 for 72 h and then exposed to 0.1 μM insulin for 30 min. The amount of GLUT4 in the plasma membrane was determined by immunoblotting analysis using anti-GLUT4 antibody.

loss of Rab4 function is involved in the decrease of GLUT4 expression in the membrane due to atorvastatin treatment.

RhoA/RhoA-Rho kinase may be another candidate for the site of action of atorvastatin since RhoA also needs geranylgeranyl pyrophosphate for lipid modification (22). In the vascular smooth muscle cell, phosphorylation of the serine residue of IRS-1 is caused by Rho kinase, a major effecter of RhoA that depresses insulin signal transduction (23). In the present study, expression of RhoA in the membrane fraction was significantly decreased, whereas that in the cytosolic fraction was significantly increased by atorvastatin (Fig. 5). Atorvastatin could cause the loss of RhoA function in 3T3L1 adipocytes. Tyrosine phosphorylation of IRS-1 and serine/threonine phosphorylation of Akt were decreased by atorvastatin in a concentration-dependent manner (Figs. 6 and 7). IRS-1 and Akt could be regulated by RhoA. The role of Akt in the insulin signal transduction is controversial. Kotani et al. (24) have demonstrated that activation of Akt is not necessary for insulin-induced glucose uptake in 3T3L1 adipocytes and that a PKCλ may be involved. Kohn et al. (25) reported that over expression of a constitutively active mutant of Akt moved GLUT4 from intracellular vesicles to the plasma membrane. Hill et al. (26) and Cong et al. (27) have been demonstrated that inhibition of Akt using dominant negative Akt, Akt antibody, or inhibitory peptides for Akt partially attenuates insulin-induced GLUT4 translocation to the membrane. Data in the present study are in accord with these findings. Since Akt phosphorylates Rab GTPase-activating protein in response to insulin (28, 29), this factor may help Rab4 to translocate GLUT4 to the plasma membrane. Insulin-induced phosphorylation of Akt could be modulated by both RhoA and Rab4.

The RhoA inactivator C3 and Rho kinase inhibitor Y27632 inhibited the insulin-induced tyrosine phosphorylation of IRS-1 (Figs. 8 and 9A). Y27632 also inhibited insulin-induced translocation of GLUT4 to the

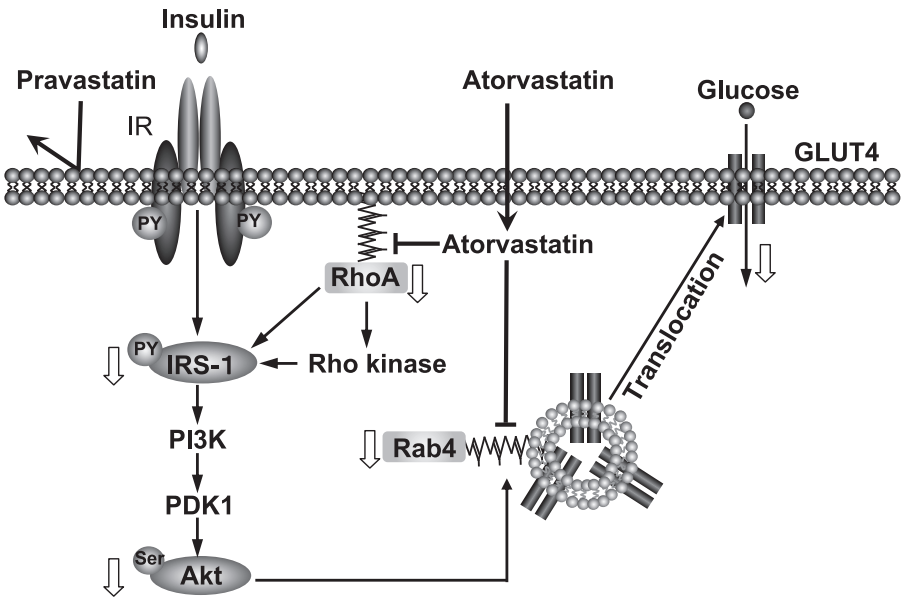

Fig. 10. Schematic representation of the insulin signaling pathway impaired by atorvastatin in 3T3L1 adipocytes. Atorvastatin can easily enter cells and inhibits synthesis of the geranylgeranyl pyrophosphate via competition with HMG-CoA reductase, leading to dysfuncion of RhoA and Rab4. RhoA and Rab4 caused by atorvastatin may disturb over-all insulin signal transduction including IRS-1 and Akt. Eventually, glucose uptake in 3T3L1 adipocytes is impaired. Pravastatin did not appreciably affect the insulin signal transduction. Open arrows indicate molecules that were impaired by atorvastatin.

plasma membrane (Fig. 9B). These results are similar to those produced by atorvastatin. It is strongly suggested that RhoA is involved in the insulin signal transduction and that dysfunction of RhoA induced by atorvastatin causes exacerbation of the response of 3T3L1 adipocytes to insulin.

We used atorvastatin and pravastatin in the present study, but we have also reported that several other hydrophobic statins, that is, atorvastatin, fluvastatin, and cerivastatin, aggravate myocardial contractile dysfunction after brief ischemia in dogs (30). In a previous study using rat vascular endothelial cells, the hydrophobic statins, atorvastatin, fluvastatin, simvastatin, lovastatin, and cerivastatin, also induced apoptotic death (31). However hydrophilic pravastatin did not influence these observations. Statins could be classified into 'useful' or 'toxic' drugs according to the membrane permeability data from our studies.

In conclusion, hydrophobic atorvastatin reduces insulin-induced glucose uptake into 3T3L1 adipocytes, resulting from attenuation of GLUT4 translocation from intracellular vesicles to the cell membrane. Insufficient supply of isoprenyl groups for RhoA and Rab4 caused by atorvastatin may disturb overall insulin signal transduction including IRS-1 and Akt. However, hydrophilic pravastatin did not appreciably affect insulin signal transduction.

References

1 Holman GD, Kasuga M. From receptor to transporter: insulin signaling to glucose transport. Diabetologia. 1997;40:991–1003.

2 Czech MP, Corvera S. Signaling mechanisms that regulate glucose transport. J Biol Chem. 1999;274:1865–1868.

3 Wada A, Yokoo H, Yanagita T, Kobayashi H. New twist on neuronal insulin receptor signaling in health, disease, and therapeutics. J Pharmacol Sci. 2005;99:128–143.

4 Vollenweider P, Martin SS, Haruta T, Morris AJ, Nelson JG, Cormont M, et al. The small guanosine triphosphate-binding protein Rab4 is involved in insulin-induced GLUT4 translocation and actin filament rearrangement in 3T3L1 cells. Endocrinology. 1997;138:4941–4949.

5 Farah S, Agazie Y, Ohan N, Ngsee JK, Liu XJ. A Rho-associated protein kinase, ROKα, binds insulin receptor substrate-1 and modulates insulin signaling. J Biol Chem. 1998;273:4740–4746.

6 Illingworth DR, Tobert JA. A review of clinical trials comparing HMG-CoA reductase inhibitors. Clin Ther. 1994;16:366–385.

7 Insull W, Kafonek S, Goldner D, Zieve F. Comparison of efficacy and safety of Atorvastatin (10 mg) with simvastatin (10 mg) at six weeks. ASSET Investigators. Am J Cardiol. 2001;87:554–559.

8 Paolisso G, Barbagallo M, Petrella G, Ragno E, Barbieri M, Giordano M, et al. Effects of simvastatin and atorvastatin administration on insulin resistance and respiratory quotient in aged dyslipidemic non-insulin dependent diabetic patients. Atherosclerosis. 2000;150:121–127.

9 Paniagua JA, López-Miranda J, Escribano A, Berral FJ, Marín C, Bravo D, et al. Cerivastatin improves insulin sensitivity and insulin secretion in early-state obese type 2 diabetes. Diabetes. 2002;51:2596–2603.

10 Rydgren T, Vaarala O, Sandler S. Simvastatin protects against multiple low-dose streptozotocin-induced type 1 diabetes in CD-1 mice and recurrence of disease in nonobese diabetic mice. J Pharmacol Exp Ther. 2007;323:180–185.

11 McGuire TF, Xu XQ, Corey SJ, Romero GG, Sebti SM. Lovastatin disrupts early events in insulin signaling: a potential mechanism of lovastatin's anti-mitogenic activity. Biochem Biophys Res Commun. 1994;204:399–406.

12 Yada T, Nakata M, Shiraishi T, Kakei M. Inhibition by simvastatin, but not pravastatin, of glucose-induced cytosolic Ca^{2+} signalling and insulin secretion due to blockade of L-type Ca^{2+} channels in rat islet β-cells. Br J Pharmacol. 1999;126:1205–1213.

13 Kanda M, Satoh K, Ichihara K. Effects of atorvastatin and pravastatin on glucose tolerance in diabetic rats mildly induced by streptozotocin. Biol Pharm Bull. 2003;26:1681–1684.

14 Knight JB, Cao KT, Gibson GV, Olson AL. Expression of prenylation-deficient Rab4 interferes with propagation of insulin signaling through insulin receptor substrate-1. Endocrinology. 2000;141:208–218.

15 Koga T, Shimada Y, Kuroda M, Tsujita Y, Hasegawa K, Yamazaki M. Tissue-selective inhibition of cholesterol synthesis in vivo by pravastatin sodium, a 3-hydroxy-3-methylglutaryl coenzyme A reductase inhibitor. Biochim Biophys Acta. 1990;1045:115–120.

16 Ichihara K, Satoh K. Disparity between angiographic regression and clinical event rates with hydrophobic statins. Lancet. 2002;359:2195–2198.

17 Yamazaki M, Suzuki H, Hanano M, Tokui T, Kamai T, Sugiyama Y. Sodium-independent multispecific anion transporter mediates active transport of pravastatin into rat liver. Am J Physiol. 1993;264:36–44.

18 Hughes AD. The role of isoprenoid in vascular smooth muscle potential benefits of statins unrelated to cholesterol lowering. J Hum Hypertens. 1996;10:387–390.

19 Goldstein JL, Brown MS. Regulation of the mevalonate pathway. Nature. 1990;343:425–430.

20 Chamberlain LH. Inhibition of isoprenoid biosynthesis causes insulin resistance in 3T3L1 adipocytes. FEBS Lett. 2001;507:357–361.

21 Cormont M, Bortoluzzi MN, Gautier N, Mari M, van Obberghen E, Le Marchand-Brustel Y. Potential role of Rab4 in the regulation of subcellular localization of Glut4 in adipocytes. Mol Cell Biol. 1996;16:6879–6886.

22 Bobak D, Moorman J, Guanzon A, Gilmer L, Hahn C. Inactivation of the small GTPase Rho disrupts cellular attachment and induces adhesion-dependent and adlhesion-indipendent apoptosis. Oncogene. 1997;15:2179–2189.

23 Begum N, Sandu OA, Ito M, Lohmann SM, Smolenski A. Active Rho kinase (ROK-α) associates with insulin receptor substrate-1 and inhibits insulin signaling in vascular smooth muscle cells. J Biol Chem. 2002;227:6214–6222.

24 Kotani K, Ogawa W, Matsumoto M, Kitamura T, Sakaue H, Hino Y, et al. Requirement of atypical protein kinase Cλ for insulin stimulation of glucose uptake but not Akt activation in 3T3L1 adipocytes. Mol Cell Biol. 1998;18:6971–6982.

25 Kohn AD, Summers SA, Birnbaum MJ, Roth RA. Expression of a constitutively active Akt Ser/Thr kinase in 3T3L1 adipocytes stimulates glucose uptake and glucose transporter 4 translocation. J Biol Chem. 1996;271:31372–31378.
26 Hill MM, Clark SF, Tucker DF, Birnbaum MJ, James DE, Macaulay SL. A role for protein kinase Bbeta/Akt2 in insulin-stimulated GLUT4 translocation in adipocytes. Mol Cell Biol. 1999;19:7771–7781.
27 Cong LN, Chen H, Li Y, Zhou L, McGibbon MA, Taylor SI, et al. Physiological role of Akt in insulin-stimulated translocation of GLUT4 in tranfected rat adipose cells. Mol Endocrinol. 1997;11:1881–1890.
28 Mîinea CP, Sano H, Kane S, Sano E, Fukuda M, Peränen J, et al. AS160, the Akt substrate regulating GLUT4 translocation, has a functional Rab GTPase-activating protein domain. Biochem J. 2005;391:87–93.
29 Larance M, Ramm G, Stöckli J, van Dam EM, Winata S, Wasinger V, et al. Characterization of the role of the Rab GTPase-activating protein AS160 in insulin-regulated GLUT4 trafficking. J Biol Chem. 2005;280:37803–37813.
30 Satoh K, Ichihara K. Lipophilic HMG-CoA reductase inhibitors increase myocardial stunning in dogs. J Cardiovasc Pharmacol. 2000;35:256–262.
31 Kaneta S, Satoh K, Kano S, Kanda M, Ichihara K. All hydrophobic HMG-CoA reductase inhibitors induce apoptotic death in rat pulmonary vein endothelial cells. Atherosclerosis. 2003;170:237–243.